# Empirical Dynamic Data Driven Detection and Tracking Using Detectionless and Traditional FiSSt Methods

Shahzad Virani[*], Timothy S. Murphy[†],
Marcus J. Holzinger[‡], and Brandon A. Jones[§]

**Abstract**

Autonomous search and recovery of resident space object (RSO) tracks is crucial for decision makers in SSA. This paper leverages dynamic data driven approaches to improve methodologies used in real-time detection and tracking of RSOs with a low signal-to-noise ratio (SNR). Detected RSOs are assigned to be tracked using one of two simultaneously operating algorithms. The Gaussian Mixture Proability Hypothesis Density (GM-PHD) filter tracks all RSOs above a certain SNR threshold, while a Detectionless Multi-Bernoulli filter (D-MB) detects and tracks low SNR objects. The D-MB filter uses matched filtering for likelihood computation which is highly non-Gaussian for dim objects. Hence, the D-MB filter is particle based which leads to higher computational complexity. The primary idea proposed in this paper is to balance the computational efficiency of GM-PHD and high sensitivity of the D-MB likelihood computation by dynamically switching tracks between the two filters based on the SNR of the target; allowing for real-time detection and tracking. These algorithms are implemented and tested on real data of objects in the geostationary (GEO) belt using a wide field-of-view camera (18.2 degrees). A star tracking mount is used to inertially stare at the GEO belt and data are collected for 2 hours corresponding to RSOs being observed in 48.2 degrees of the GEO belt.

## 1 Introduction

Space Domain Awareness (SDA) is the ability to detect, track, and categorize space objects.[1] Though the current space object catalog houses over 20,000 objects, the database is far from complete and the number of space objects in orbit is increasing. New objects need to be detected, and known objects in the catalog need to be maintained and updated as they drift due to orbital perturbations.[2,3] To successfully incorporate the data, SDA relies on sensor development, algorithm development, network development, tasking development, and data sharing.[4] Together, these allow the tracking and characterization of passive and active space objects.

Space surveillance systems, such as telescopes and radar observations, have the capability of detecting and tracking space objects, but by using the visible light spectrum are limited by atmospheric conditions and night operations.[5] Though optical telescopes, with narrow field of view,

[*]Graduate Student, Daniel Guggenheim School of Aerospace Engineering, Georgia Institute of Technology.
[†]Graduate Student, Daniel Guggenheim School of Aerospace Engineering, Georgia Institute of Technology.
[‡]Assistant Professor, Daniel Guggenheim School of Aerospace Engineering, Georgia Institute of Technology.
[§]Assistant Professor, Department of Aerospace Engineering and Engineering Mechanics, University of Texas at Austin.

provide better resolution imagery of the space objects, they are limited to a few space objects in a portion of the sky at a time. Objects in LEO also provide a challenge for ground based systems, as the objects have a greater angular rate unlike objects in GEO, which have a slower angular rate and remain in the same area of the sky for a longer duration.[6]

Space objects can be detected and tracked using various phenomenologies including radar or optical methods.[4] This paper will only focus on optical methods. However, the theory can be extended for other phenomenologies. First, image processing algorithms analyze the images to classify objects as stars, RSOs, or artifacts (hot or dead pixels). These objects can take the form of either a point or a streak depending on the type of sensor, exposure time, and relative angular velocities of the objects.[7] After an object is detected, the object is tracked from frame-to-frame after which the orbital parameters can be estimated, most classically with the method of Gauss using three observations of the same object at different moments in time.[6]

Objects can be detected then tracked, or tracked and detected simultaneously. Detect-before-track methods threshold images and test detected objects and corresponding positions with velocity matching methods.[8] Using a star catalog, a mask can be applied to a single frame leaving dimmer stars and potential RSOs behind.[7] Levesque applies a match filtering technique to identify streaks during a reacquisition of data where the image astrometry is known. In this situation, the sensor accesses an RSO database housing a description of the objects' mean orbital parameters to retrieve the RSO's angular rates and direction.

Once the stars in an image are eliminated, the matched filter is applied to identify streaks and obtain the RSOs exact location.[9] Once detected, the RSOs are then tracked and associated from frame to frame. Methods such as Multiple Target Indicator (MTI) and Multiple Hypothesis Tracking (MHT) have already been used to track multiple objects in the image. Observation probabilities can also be integrated into the track association process. For example, Mohanty applies a maximum likelihood algorithm, to estimate the changing mean and covariance of the assumed Gaussian background to detect RSOs.[10]

Though detect-before-track methods, such as MTI and MHT, are generally computationally efficient, they do not perform well in dimly lit conditions. Alternatively, track-before-detect methods evaluate multiple frames and uses the raw measurements to simultaneously detect objects and evaluate their motion.[3] Various methods have been developed to detect and track low SNR signals, such as shift and add methods,[11] multi-object tracking,[12] and multi-frame matched filters.[13] Recently, much work has been done on Random-Finite Set (RFS) based filters, particularly in the area of computer vision. Particle filter implementation of these RFS-based filter approaches such as, Probability Hypothesis Density approach (PHD)[14] filter and Generalized Labeled Multi-Bernoulli Filters (GLMB)[15] [16] , have also been developed. One of the disadvantages of these particle filter based methods is their heavy use of computational resources and time, especially for wide field-of-view cameras with multiple tracks.

The motivation behind this paper is to use image processing techniques and prior information from the Two Line Elements (TLEs) to perform an informed search on an image from wide field-of-view sensor. Once the known space objects are detected, a blind search is then conducted on the rest of the image to detect unknown space objects. The detected objects from both methods can then be tracked using GM-PHD along with MHT (for high SNR signals) and D-MB (for low SNR signals) from frame-to-frame. This paper contains the following elements: 1) a brief introduction of space object detection using matched filter templates and the Matched Filter based likelihood function 2) informed and blind search using matched filters on wide field-of-view (fov)

imagery, 3) multi-target tracking using GM-PHD along with MHT and D-MB, and 4) automatic switching between GM-PHD along with MHT and D-MB filters based on the SNR of the signal for computational efficiency.

# 2 Theory

## 2.1 Detection via Threshold

A simple way to detect objects in images is via thresholding. Thresholding considers a detection to be any pixel or pixel group which has pixel values above an intensity threshold. Groups of pixels which appear to come from the same object are then used to compute a centroid which is used as the measurement location.

The threshold can be chosen in a variety of different ways, dependent on the tracking method. This paper will choose the detection threshold based on SNR. A pixel value in an image is computed by integration of photon counts from a portion of the sky for a certain period of time. Hence, the integration time interval is defined as follows, where $t_I$ is the duration of the exposure.

$$\mathcal{T} = [t_0, t_0 + t_I] \tag{1}$$

Let a measurement $\boldsymbol{Z}(t_0, t_I) \in \mathbb{Z}^{d_1 \times d_2}$ be a matrix of pixel values representing an image. The value of pixel $z_j$ is dependent on the integration time and will contain a mean signal $\mu_j$ and zero mean Gaussian read noise $w_j$.

$$\begin{aligned} z_j(\mathcal{T}) &= \mu_j + w_j \\ w_j &\sim \mathcal{N}(0, \sigma_{w,j}^2) \end{aligned} \tag{2}$$

Due to the light pollution and brightness of the sky, a real image will contain noise that is not zero mean, requiring background subtraction before using matched filters.[17] The implementation of background subtraction will be further discussed in the Approach section. The signal to noise ratio in a pixel $z_j$ is then the expected value of the signal over the standard deviation of the noise,

$$\begin{aligned} \text{SNR}(z_j(\mathcal{T})) &= \frac{\mathbb{E}[z_j(\mathcal{T})]}{\sqrt{\mathbb{E}[z_j(\mathcal{T}) - \mathbb{E}[z_j(\mathcal{T})])^2]}} \\ &= \frac{\mu_j(\mathcal{T})}{\sigma_{w,j}} \end{aligned} \tag{3}$$

In a given pixel, the detected SNR in pixel $j$ is calculated using $z_j$ instead of $\mu_j$. Hence, the SNR threshold is the number of standard deviations over the mean a pixel needs to reach in order to be considered a detection. Higher SNR threshold prevents more false detections, but will fail to consistently detect dimmer objects. Hence, SNR threshold is inherently tied to the number of false alarms, and clutter statistics, which are used in the filter process.

## 2.2 Detection via Matched Filter

This section summarizes important concepts of matched filtering. Filter template generation for the space objects from their Two Line Elements (TLEs) will be discussed in the Approach section.

The matrix of pixels can be decomposed into a signal matrix and a noise matrix as follows

$$\begin{aligned} \boldsymbol{Z}(\mathcal{T}) &= \boldsymbol{M}(\mathcal{T}) + \boldsymbol{W}(\mathcal{T}) \\ \boldsymbol{M}(\mathcal{T}) &\in \mathbb{Z}^{d_1 \times d_2}, \boldsymbol{W}(\mathcal{T}) \in \mathbb{Z}^{d_1 \times d_2} \end{aligned} \tag{4}$$

A matched filter is predicated on a hypothesized signal structure, also known as a template, $\boldsymbol{M_0}(\mathcal{T}) \in \mathbb{Z}^{d_3 \times d_4}$. $\boldsymbol{M_0}(\mathcal{T})$ contains a hypothesis of the signal in $\boldsymbol{M}(\mathcal{T})$. A matched filter can be defined as a mapping $g_{MF} : \mathbb{Z}^{d_1 \times d_2} \times \mathbb{Z}^{d_3 \times d_4} \rightarrow \mathbb{Z}^{d_1 \times d_2}$.

$$\boldsymbol{Z}'(\mathcal{T}) = g_{MF}(\boldsymbol{Z}(\mathcal{T}, \boldsymbol{M_0}(\mathcal{T}))) \tag{5}$$

This function is a discrete convolution of $\boldsymbol{M_0}(\mathcal{T})$ centered on $z_j \in \boldsymbol{Z}(\mathcal{T})\ \forall j$. The result of this convolution is the correlation between the template and the signal. If the template signal is identical to the measured signal, then the result of the convolution is maximized. The results can be normalized such that a perfect positive correlation between the template and the signal is equal to one and a perfect anti-correlation is equal to negative one. A few key definitions are also important for analyzing the results from matched filtering. The pixel-wise SNR for a particular pixel, $z_j(\mathcal{T})$ is defined in Equation (3). Similarly, the total object SNR is defined as

$$\begin{aligned} \text{SNR}\left(\sum z_j(\mathcal{T})\right) &= \frac{\mathbb{E}\left[\sum z_j(\mathcal{T})\right]}{\sqrt{\mathbb{E}[(z_j(\mathcal{T}) - \mathbb{E}[z_j(\mathcal{T})])^2]}} \\ &= \frac{\sum \mu_j(\mathcal{T})}{\sqrt{\sum \sigma_{w,j}^2}} \\ &= \sqrt{n_z}\frac{\bar{\mu}_j(\mathcal{T})}{\sigma_w} \end{aligned} \tag{6}$$

where $n_z$ is the number of pixels associated with the signal from the object of interest, $\bar{\mu}_j$ is the average of all the signal values from the pixels, and $\sigma_w$ is the average per pixel noise in the image. Additional details about matched filtering can be found in a paper by Murphy et. al.[18] The matched filter result can be used as a direct detection technique by thresholding the results of the matched filter. This paper will also use the matched filter as a likelihood function for a particle based filter

### 2.3 Detection via Matched Filter Likelihood Function

This section reviews the likelihood function being used in this paper, first proposed by Murphy et al.[19] The measured signal in pixel $i$ is assumed to be zero mean noise, $w_i$, and signal, $h_i(\mathbf{x})$, generated by space object with a state $\mathbf{x}$. The matched filter template can be written as a list of pixels predicted to have signal, $T(\mathbf{x})$, and the predicted values in those pixels, $h_i(\mathbf{x})$. The matched filter is the weighted sum of the measured pixels, $z_i$, weighted by the predicted values, $h_i(\mathbf{x})$,

$$z_{MF} = \sum_{i \in T(\mathbf{x})} a h_i(\mathbf{x}) z_i = 0 \tag{7}$$

where $a$ is an arbitrary scaling factor. In particular, $a$ represents the fact that, while we can predict the relative values of the pixels, we often cannot predict the total brightness of an object.

The noise is commonly assumed to be Gaussian distributed, which simplifies the following discussion. Because the noise, $w_i$, is assumed to be a mean zero signal, if the predicted region

contains no signal, $h_i(\mathbf{x}) = 0 \; \forall \, i \in T(\mathbf{x})$, the resulting distribution is mean zero,

$$\mathbb{E}[z_{MF}|s_i = 0] = a \sum_{i \in T(\mathbf{x})} h_i(\mathbf{x}) E[w_i] = 0 \tag{8}$$

$$\text{Var}[z_{MF}] = \mathbb{E}\left[\left(a \sum_{i \in T(\mathbf{x})} h_i(\mathbf{x}) w_i\right)^2\right] = a^2 \sigma_w^2 \sum_{i \in T(\mathbf{x})} h_i^2(\mathbf{x}) \tag{9}$$

$$z_{MF} \sim \mathcal{N}(\alpha^2, a^2 \alpha^2 \sigma_w^2) \tag{10}$$

By a similar argument, if there is signal content in the pixels on which the matched filter operates, the result has a mean greater than zero. The measured matched filter result then has a distribution with known expected value and variance,

$$\mathbb{E}[z_{MF}|s_i = h_i(\mathbf{x}_{true})] = a \sum_{i \in T(\mathbf{x})} h_i(\mathbf{x}) h_i(\mathbf{x}_{true}) = a\alpha^2 \tag{11}$$

The matched filter result, $z_{MF}$, can be assumed to exist in one of two distributions

$$\tilde{\phi}(z) = \mathcal{N}(z; 0, a^2 \alpha^2 \sigma_w^2) \tag{12}$$

$$\tilde{\psi}(z; \beta) = \mathcal{N}(z; \beta, a^2 \alpha^2 \sigma_w^2), \;\; \beta > 0 \tag{13}$$

Recall that the typical matched filter assumes that noise is i.i.d., which is violated by shot noise which is explicitly dependent on the magnitude of the signal. Because signal magnitude is unknown, shot noise must either be estimated or ignored. Typically, for low SNR signals, shot noise is dominated by other noise sources and can be ignored. If estimated, it will require calculation of the covariance matrix $\mathbf{R}_w$.This is a limitation of the current method.

Next, the following null and alternate hypotheses for a binary hypothesis test are defined as[20]

$$\begin{aligned} H_0 &: z \sim \tilde{\phi}(z) \\ H_1 &: z \sim \tilde{\psi}(z; \beta); \beta = z_{MF}. \end{aligned} \tag{14}$$

This test assumes $T(\mathbf{x})$ contains no signal, and tests whether the measurement gives significant evidence to challenge that hypothesis. For binary hypothesis testing, a probability of false alarm is set, $p_{FA}$, which in turn defines an integration threshold, $z_{TH}$, based on the null hypothesis cumulative density function (CDF).

$$p_{FA} = \int_{z_{TH}}^{\infty} \tilde{\phi}(z) dz \tag{15}$$

A probability of detection can be calculated with the following integral.

$$p_D = \int_{z_{TH}}^{\infty} \tilde{\psi}(z) dz \tag{16}$$

This hypothesis test determines if there is significant evidence that the predicted signal exists in the predicted location. Because the matched filter gives a SNR gain, this test should maximize $p_D$, though an explicit proof of this claim has not yet been shown.

The probability of existence update can also be formulated in terms of the matched filter. The relative likelihood can be calculated from the two distributions in Equation (13). This leads to the particle-wise relative likelihood

$$g_z(\mathbf{x}) = \frac{\tilde{\psi}(z_{MF})}{\tilde{\phi}(z_{MF})} \tag{17}$$

These equations provide everything needed to update particle weights in a Bayesian or Bernoulli filter.

### 2.4 Multiple Hypothesis Tracking

Multiple hypothesis tracking (MHT) attempts to solve the multiple assignment problem by deferring the assignment until enough information is available to make a decision with certainty. MHT tracks are initiated by considering three cases for each measurement in each frame:
1. The observation starts a new track.
2. The observation updates an existing track.
3. The observation is following a skipped observation for an existing track.[21]

Over the series of $k$ frames, the current implementation of MHT uses a Kalman Filter to generate a tree of such hypotheses or possible tracks based on the observations. Each track has a probability associated based on the estimated state and covariance matrices. The presented implementation of MHT recomputes the hypotheses with each new frame, maintaining only the tracks and scores from frame $k-1$.

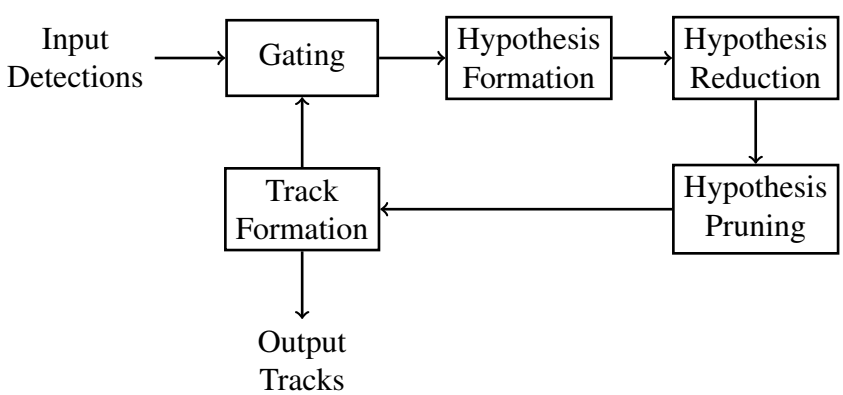


Figure 1: Track Oriented MHT Logic Diagram

In the gating step, the covariance is used to provide the probability of the updated state of a track based on its dynamics and the new measurement. A hypothesis is formed after gating a new observation with each track using the Mahalanobis distance. In addition to potentially appending measurements in a current frame to the current tracks, additional hypotheses are made for the scenario of a track skipping an observation in the frame and for a current measurement beginning an independent track. Once the hypotheses are formed, the track score and observation probabilities are calculated based on the probability of detection and density of false alarms. Hypotheses are

then reduced if the track score falls underneath a predetermined track score threshold. After all the hypotheses are formed, they are sorted in descending order of likelihood ratio and the algorithm selects the most probable track for each measurement in a frame. The tracks are then pruned by deleting hypotheses that conflict with the newly identified tracks. This process is repeated for each new frame. The exact implementation with equations is further discussed by Lee et al.[22]

### 2.5 Multi-Bernoulli Filter

This section briefly describes the theory behind multi-Bernoulli Filters. An in-depth discussion of the theory and implementation is further discussed by Vo et al.[23] and Murphy et al.[24] Understanding the Bernoulli filter begins with Bayesian filtering equations as follows:

$$\pi_{k|k-1}(\boldsymbol{x}_k|\boldsymbol{z}_{1:k-1}) = \int f(\boldsymbol{x}_k|\boldsymbol{x}_{k-1})\pi_{k-1}(\boldsymbol{x}_{k-1}|\boldsymbol{z}_{1:k-1})d\boldsymbol{x}_{k-1} \tag{18}$$

$$\pi_k(\boldsymbol{x}_k|\boldsymbol{z}_{1:k}) = \frac{g(\boldsymbol{z}_k|\boldsymbol{x}_k)\pi_{k|k-1}(\boldsymbol{x}_k|\boldsymbol{z}_{1:k-1})}{\int g_k(\boldsymbol{z}_k|\boldsymbol{x})\pi_{k|k-1}(\boldsymbol{x}|\boldsymbol{z}_{1:k-1})d\boldsymbol{x}} \tag{19}$$

where $\boldsymbol{z}_k$ represents the measurements until time-step $k$. Equations 18 and 19 and prediction and update step equations, respectively. For a Bernoulli filter, the state is instead modeled as a Bernoulli random finite set (BFRS). The parameter set, denoted by $\mathcal{S}_k$ contains a random finite set containing one object with a probability $r_k$. Hence, the probability of the set being empty is $1-r_k$. The spacial distribution of the object in the set is described by a PDF, $p(\boldsymbol{x_K})$, and probability of existence:

$$\mathcal{S} = \{p(\boldsymbol{x}_k, r_k)\} \tag{20}$$

The PDF is estimated using equations 18 and 19 and updates the probability of existence using equations from a paper by Vo et al.[23] The update equations for a multi-target tracking are as follows:

$$\pi_{k|k-1}(\chi_k|\boldsymbol{z}_{1:k-1}) = \int f_{k|k-1}(\chi_k|\chi)\pi_{k-1}(\chi_k|\boldsymbol{z}_{1:k-1})\partial\chi \tag{21}$$

$$\pi_{k|k-1}(\chi_k|\boldsymbol{z}_{1:k}) = \frac{g(\boldsymbol{z}_k|\chi_k)\pi_{k|k-1}(\chi_k|\boldsymbol{z}_{1:k-1})}{\int g(\boldsymbol{z}_k|\chi_k)\pi_{k|k-1}(\chi|\boldsymbol{z}_{1:k-1})\partial\chi} \tag{22}$$

where $g(\cdot|\cdot)$ is the likelihood function. The distribution $\pi_k$ is a multi-object belief function and is similar to a PDF in that higher density means higher probability of an object existing in that area. However, $\pi_k$ does not need to integrate to 1. Instead, the total mass of an area is the expected number of objects in that area.[24]

For a multi-object filter, $\chi_k$ is random finite set used to represent the multi-object tracking problem where the number of objects is unknown. The multi-Bernoulli filter represents the multi object state as the union of a series of BRFSs. Instead of using the likelihood function by Vo et al,[23] this paper will be using the matched filter based likelihood function as discussed in prior section.

Two likelihood functions are used in this paper in conjunction with a multi-Bernoulli filter. When using thresholding as the measurement source, each detection is used as a unique measurement input to the filter. Each measurement is assumed to be spatially distributed with a Gaussian distribution centered at the detection centroid. Many such detections are false alarms from either the noise or undetected stars in the background; a Bernoulli filter models this with a clutter model. Because the noise sources are Gaussian distributed, this filter can use a Gaussian approximation

for the spacial distribution of the tracked objects. In particular, this work will employ a Gaussian mixture approximation of the multi-object belief function.

The second likelihood function used in the paper is matched filter likelihood function. This likelihood requires a matched filter template, which in turn requires a state hypothesis. This likelihood function, as such, is defined for every point in the state space and, in the case of dim objects, can be highly non-Gaussian. As such, a full particle filter is needed to run a filter with this likelihood, leading to a much higher computational complexity. The benefit is that the matched filter provides an inherent SNR gain allowing much dimmer objects to be tracked.

The primary driving idea in the algorithms proposed in this paper is to balance the computational efficiency of a Gaussian approximation filter and the high sensitivity of the matched filter likelihood. The Gaussian mixture multi-Bernoulli filter attempts to track all objects above a certain SNR threshold. The matched filter multi-Bernoulli filter then tracks all objects that the previous filter failed to detect. The tracks between the two filters are switched based on the photometric SNR of the target being tracked. This interchangeability between the filters is dependent on the distibutions being interchangeable between a particle approximation and a Gaussian mixture approximation.

### 2.6 Gaussian Mixture - Probability Hypothesis Density Filter

One of the drawbacks of the Sequential Monte Carlo approximation of the Probability Hypothesis Density filter[14] is that it requires a large number of particles, which significantly increases the computation time. Additionally, since it's a multi-target filter, the state estimates are often extracted using clustering techniques. These techniques often require the number of objects that are being tracked. The cardinality of the set computed using the weights can be used to approximate the number of objects, but it is not as reliable in cases where new objects appear in the frame or objects leave the frame. The Gaussian Mixture - PHD filter, proposed by Vo and Ma,[25] attempts to solve both of these problems. The fundamental difference is that the GM-PHD filter propagates an intensity using PHD recursion and it does not require clustering algorithms to estimate the states. The derivation of equations and implementation of this filter is covered in detail by Vo and Ma.

However, the GM-PHD filter has one drawback. Even though it tracks multiple objects from frame-to-frame, it is unable to generate track information, i.e. associate the state estimates and generate new tracks between frames. To generate track information, MHT is used as an associate filter with the GM-PHD state estimates, i.e. GM-PHD is used as a pre-clutter filter for MHT. This approach takes the output of the GM-PHD filter and performs data association on them. For each image, the filter outputs an estimate of the number of targets as well as their states. This output from the filter is used as new observation model for MHT in the following manner:

$$\tilde{y}_{k,i} = x_{k,i} + n_{k,i} \;\; i = 1, \ldots N \tag{23}$$

where $k$ is the time-step or image index and $N$ is the estimated number of targets. Panta et al[26] estimate the statistics of the noise $n_{k,i}$ as a zero-mean Gaussian process with variance $Q_{k,i}$. With this approach, regardless of the fact that the observation process is non-linear or non-Gaussian, the data-association functionality is given a linear observation process. Moreover, since the GM-PHD is used as pre-clutter filter, the pruning of the track hypotheses is simpler in this approach than just MHT due to significantly less number of hypotheses generated.

## 3 Approach

This section discusses the overall approach used including image processing algorithms, tracking, and matched filtering on a real image data.

The dataset for this research was collected using a 85 mm $f/1.2$ lens and a 16-bit 12.2 megapixel sensor. The effective field-of-view of the imaging system was 15.2° x 10.1°. In order to survey the GEO belt, a tracking mount was used to tracks the stars. Hence, the stars remain stationary while the space objects in GEO move through the field-of-view. The setup for the imaging system is shown in Figure 2. The images were taken with 5 seconds integration time and 1 second delay between the frames. 994 frames were taken which resulted in 48.2° coverage of the GEO belt in approximately 100 minutes. Since the dataset was taken during the specular (glint) season, the objects became brighter and dimmer as they moved into the Earth's shadow.

Figure 2: Image of the setup for the data capture.

A real image has multiple sources of noise. In order to use the theories discussed above, it is important that the images are processed such that the noise in the image is zero mean. Typically, the sensor has some hot pixels and bias. To mitigate this effect in the image, several frames are taken with the iris of the lens closed with the same integration time as the observations. An average dark frame is computed and subtracted from every image that is taken from the sensor and is known as dark frame subtraction. Additionally, the brightness of the sky varies in the image. Usually,

the portion of the sky above the zenith is darker than the horizon, although it varies based on the location of the moon. Hence, a median background is estimated using non-linear least squares that captures the variation of the sky brightness in the image. This process is performed on all of the images and is known as background subtraction.

Once the dark frame and the background frame are subtracted, the signals left in the image must only be from point sources. These can include stars, space objects, airplanes, etc. While performing matched filtering to detect low SNR signals, if the template is convolved with a bright star, the result will be a bright streak. Hence, the stars must be subtracted from the image. There are several ways to accomplish star subtraction. One of the ways is to use convex optimization to perform star subtraction.[27] Another alternative is to register the stars in the image to a star catalog and delete the point sources from the image. Often in SSA, the object is being tracked using a tracking mount and the stars appear as streak in the images. For these cases, a star template can be generated using the location and the angular velocity from the tracking mount. A matched filter can then be used to detect the locations of the stars and can be subtracted based on their matched filter score.

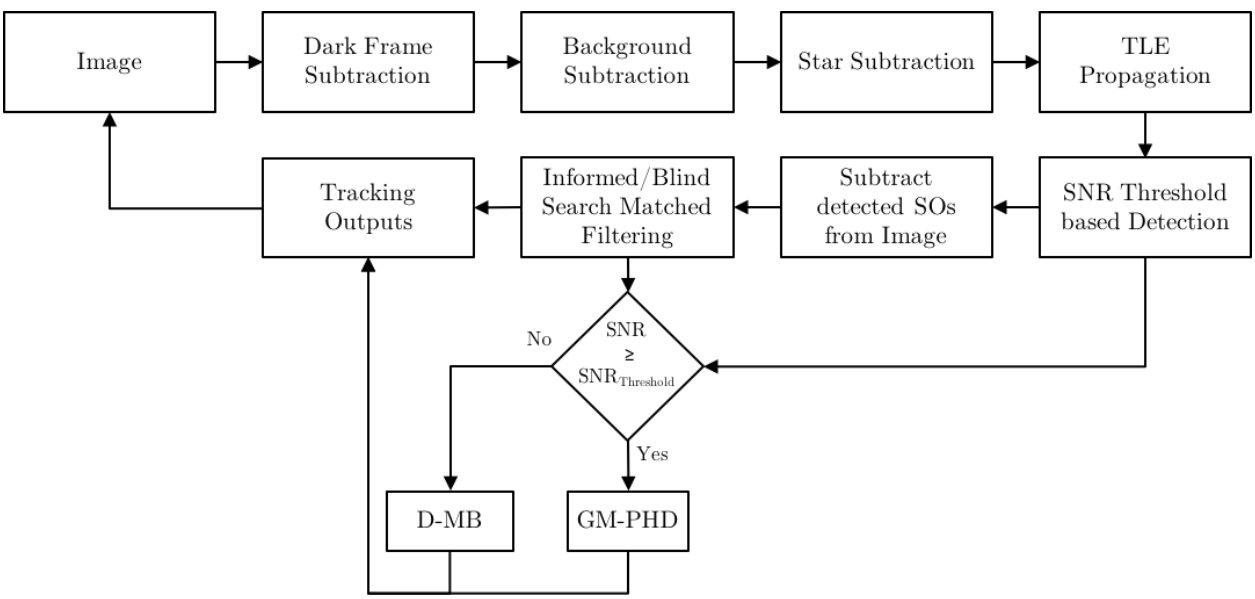


Figure 3: Block diagram discussing overall procedure for detection and tracking.

After star subtraction, the public space object catalog is propagated to the beginning of the exposure. Since the latitude, longitude, and the field-of-view of the sensor are known, the space objects that must be detectable in the frame are identified. These space objects are propagated until the end of the exposure to determine their expected streak length, location, and orientation in the image and templates for all these space objects are generated. Then point sources are detected in the image above a given *pixelwise* SNR threshold. These measurements are then passed to the GM-PHD filter for tracking. Data association between the state estimates of GM-PHD & MHT filter and expected TLE states gives a list of all expected space objects that were not detected. These objects are cued for informed search matched filtering in D-MB filter. Additionally, the PSF of these bright objects are also subtracted from the image to prevent the two filters from tracking the same object.

Now, the only signals left in the image are from unknown space objects. A series of templates are then generated with different streak lengths and orientations to detect any unknown objects in the image. If the *photometric* SNR of the signal detected is greater than or equal to $\text{SNR}_{threshold}$, the object location is passed to GM-PHD filter for tracking. If not, then each object location is passed to a D-MB filter for tracking. After the tracking step is complete, the predictions for all the objects are then fed back into the next dataset and this process is repeated. The overall approach used in this paper is summarized in Figure 3.

# 4 Results

This section shows some of the preliminary results from the use of the above mentioned algorithms. Figure 4 shows a portion of a raw image from the dataset. This contains the dark noise and background noise along with the stars (clutter). The image is inverted for better visibility on paper. Dark frame and background is subtracted for the same image and is shown in Figure 5 and the space objects are now clearly visible.

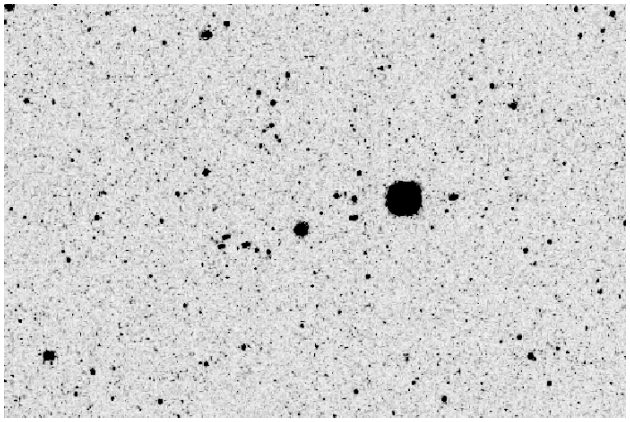

Figure 4: A portion of the raw image from the dataset.

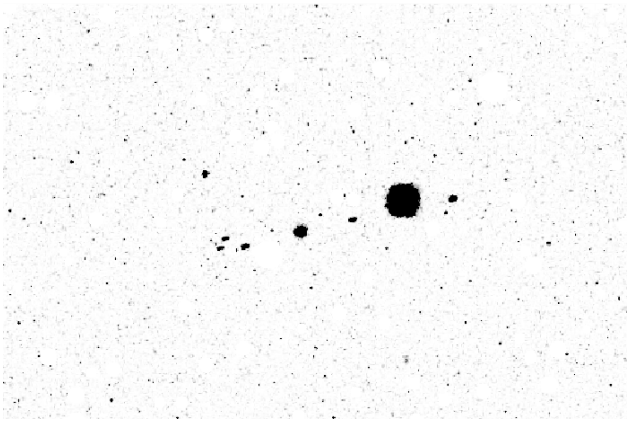

Figure 5: Image after dark frame subtraction, background subtraction, and star subtraction.

Figure 6 shows the cardinality, an estimate of the number of targets in each image, for both the GM-PHD with MHT and D-MB filters. GM-PHD with MHT does well with tracking the high

SNR targets in the dataset. The D-MB filter is able to track roughly 6 low SNR objects in part of the dataset.

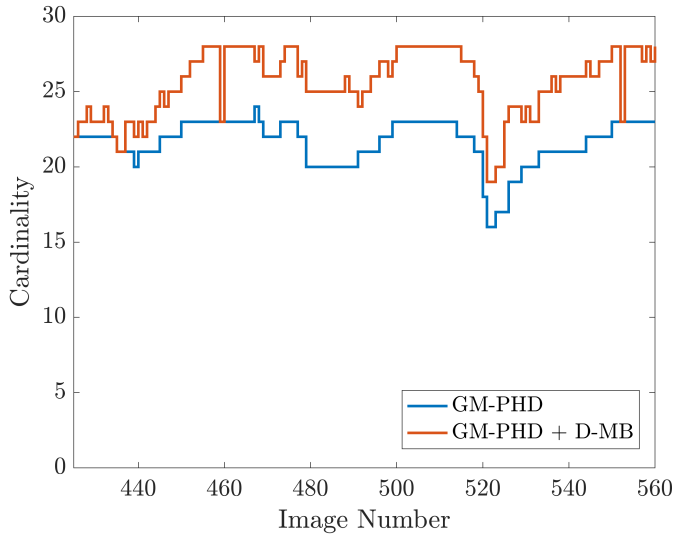


Figure 6: Comparision of the cardinality from both filters.

Figure 7 shows the photometric SNR of a particular object that was tracked by the D-MB filter in part of a dataset. The PSF for this dataset was within 10 x 10 pixels. Hence, the number of pixels associated with signal from an object was roughly 80-100 pixels. From equations 6 and 3, the photometric SNR of an object increases by $\sqrt{n_z}$ from the pixelwise SNR, where $n_z$ is the number of pixels contributing to the signal. Therefore, the pixelwise SNR of the object shown goes below 1 in some frames. Figure 8 shows the probability of existence of the same object over part of a dataset. The probability of existence of the object varies less than the photometric SNR. Therefore, the filter is able to track the object well even though the pixelwise SNR of the object is below 1.

However, one of the limitations of the DM-B filter is the amount of computation time it takes for each image. Since the D-MB is particle based and the likelihood function is highly non-Gaussian for low SNR objects, a lot of particles are needed for tracking per filter. Additionally, the PSF of an object in this dataset is about 10 x 10 pixels, while the entire image is 12.2 megapixels. So a lot of Bernoulli filters are require to mine the image for unknown space objects, which drastically increases the runtime. However, the filters can be parallelized for computational efficiency and runtime. Additionally, the images can also be binned to provide better photometric characteristics and lower resolution images.

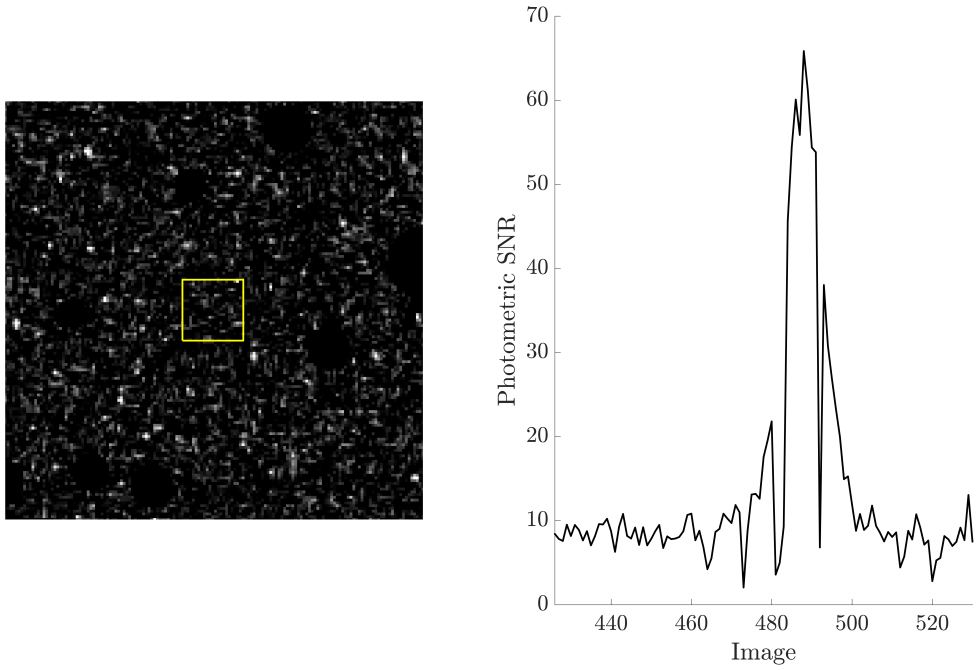


Figure 7: Plot of Photometric SNR of an object tracked using D-MB filter.

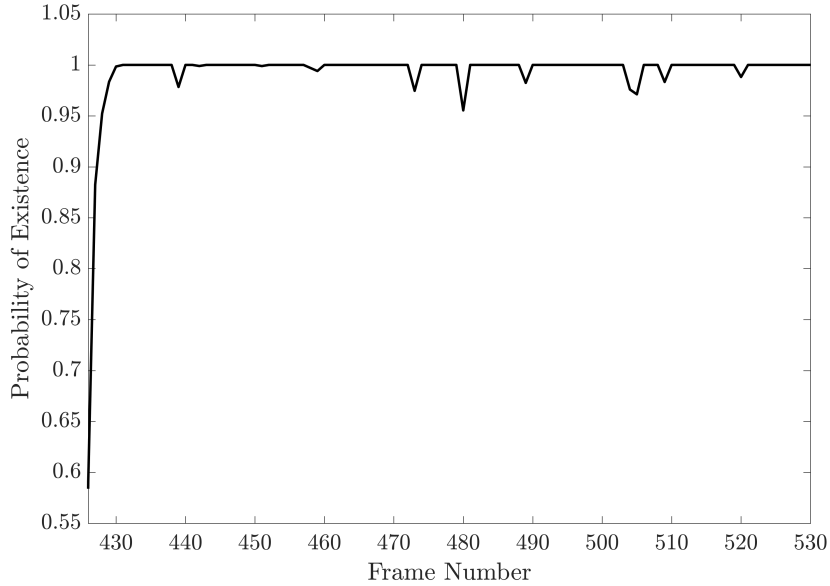


Figure 8: Probability of existence of the object over consecutive frames .

## 5 Conclusion

This main objective of this paper was to improve on the methodologies used in low SNR detection and tracking. First, image processing methods, such as dark frame subtraction and background subtraction, are used to reduce the noise in the image. Star subtraction is then performed to eliminate bright point sources in the image. Space object catalog is then propagated to generate templates for detection. A pixel-wise SNR based threshold is used for detecting targets with high SNR. These detections are then tracked using GM-PHD. Since the GM-PHD does not output track information, GM-PHD is used a pre-clutter filter for MHT to generate tracks. Data association is performed with the state estimates of the tracks and the TLE catalog. The untracked space objects are then cued for detection and tracking using D-GMB filter. Tracks are switched between the two filters based on the photometric SNR of the targets. These algorithms are also tested on real data of objects in the geostationary belt from a wide field-of-view sensor.

There are numerous potential extension to this work. First, the current implementation of the D-MB filter is not parallelized, even though the theory states it is embarrasingly parellel since there is no information exchange between two Bernoulli filters. This should signifcantly improve the run time, allowing for real time tracking. Additionally, it would also allow detectionless tracking of more low SNR objects. Second, a Generalized-Labeled Multi-Bernoulli (GLMB) filter, which is currently the state-of-the-art, provides a framework to track mulitple high SNR objects with track information. Hence, a GLMB instead of the GM-PHD along with MHT is more suitable for this work.

## References


[1] Tyler J. Hardy and Stephen C. Cain. Characterizing point spread function (psf) fluctuations to improve resident space object detection (rso). volume 9469, pages 946904–946904–10, 2015.

[2] T. Blake, M. Goergen, M. Sanchez, S. Sundbeck, and J. Krassner. DARPA Space Domain Awareness. In *Advanced Maui Optical and Space Surveillance Technologies Conference*, page 39, September 2012.

[3] M. Fanaswala and V. Krishnamurthy. Syntactic models for trajectory constrained track-before-detect. *Signal Processing, IEEE Transactions on*, 62(23):6130–6142, Dec 2014.

[4] A. Ciurte, A. Soucup, and R. Danescu. Generic method for real-time satellite detection using optical acquisition systems. In *Intelligent Computer Communication and Processing (ICCP), 2014 IEEE International Conference on*, pages 179–185, Sept 2014.

[5] M. Mallick, S. Rubin, and Ba-Ngu Vo. An introduction to force and measurement modeling for space object tracking. In *Information Fusion (FUSION), 2013 16th International Conference on*, pages 1013–1020, July 2013.

[6] Turcu V. A Danescu R, Ciurte A. A low cost automatic detection and ranging system for space surveillance in the medium earth orbit region and beyond. *Sensors (Basel)*, 2014.

[7] Thomas Schildknecht Edith Stoveken. Algorithms for the optical detection of space debris objects. In *Proceedings of 4th European Conference on Space Debris*, 2005.

[8] Peter S. Gural, Jeffrey A. Larsen, and Arianna E. Gleason. Matched filter processing for asteroid detection. *The Astronomical Journal*, 130(4):1951, 2005.

[9] Martin P. Levesque. Automatic reacquisition of satellite positions by detecting their expected streak in astronomical images. Technical report, Defence R&D Canada, 2009.

[10] N. C. Mohanty. Computer tracking of moving point targets in space. *IEEE Trans. Pattern Anal. Mach. Intell.*, 3(5):606–611, May 1981.

[11] Chengxing Zhai, Michael Shao, Bijan Nemati, Thomas Werne, Hanying Zhou, Slava G. Turyshev, Jagmit Sandhu, Gregg Hallinan, and Leon K. Harding. DETECTION OF a FAINT FAST-MOVING NEAR-EARTH ASTEROID USING THE SYNTHETIC TRACKING TECHNIQUE. *ApJ*, 792(1):60, aug 2014.

[12] Ronald PS Mahler. *Statistical multisource-multitarget information fusion*. Artech House, Inc., 2007.

[13] Irving S Reed, Robert M Gagliardi, and Larry B Stotts. A recursive moving-target-indication algorithm for optical image sequences. *Aerospace and Electronic Systems, IEEE Transactions on*, 26(3):434–440, 1990.

[14] Ba-Ngu Vo, Sumeetpal Singh, and Arnaud Doucet. Sequential monte carlo methods for multitarget filtering with random finite sets. *Aerospace and Electronic Systems, IEEE Transactions on*, 41(4):1224–1245, Oct 2005.

[15] R. Mahler. Statistics 102 for multisource-multitarget detection and tracking. *Selected Topics in Signal Processing, IEEE Journal of*, 7(3):376–389, June 2013.

[16] Stephan Reuter, Ba-Tuong Vo, Ba-Ngu Vo, and Klaus Dietmayer. The labeled multi-bernoulli filter. *IEEE Transactions on Signal Processing*, 62(12):3246–3260, jun 2014.

[17] Y. Benezeth, P. M. Jodoin, B. Emile, H. Laurent, and C. Rosenberger. Review and evaluation of commonly-implemented background subtraction algorithms. In *Pattern Recognition, 2008. ICPR 2008. 19th International Conference on*, pages 1–4, Dec 2008.

[18] T. Murphy, M. Holzinger, and B. Flewelling. Visual tracking methods for improved sequential image-based object detection. *Journal of Guidance, Control, and Dynamics (Submitted)*, 2016.

[19] Timothy S. Murphy, Marcus J Holzinger, and Brien Flewelling. Space object detection in images using matched filter bank and bayesian update (submitted). *Journal of Guidance, Control, and Dynamics*, 2016.

[20] Douglas C Montgomery and George C Runger. *Applied statistics and probability for engineers*. John Wiley & Sons, 2010.

[21] Angelos Amditis, George Thomaidis, Pantelis Maroudis, Panagiotis Lytrivis, and Giannis Karaseitanidis. Multiple hypothesis tracking implementation. In *Laser Scanner Technology*. InTech, Mar 2012.

[22] J. Lee, L. Zubair, S. Virani, T. Murphy, and M. Holzinger. Hardware-in-the-loop comparison of space object detection and tracking methodologies. In *26th AIAA/AAS Spaceflight Mechanics Meeting Napa CA*, 2016.

[23] Ba-Ngu Vo, Ba-Tuong Vo, Nam-Trung Pham, and David Suter. Joint detection and estimation of multiple objects from image observations. *IEEE Transactions on Signal Processing*, 58(10):5129–5141, oct 2010.

[24] Timothy S Murphy, Marcus J Holzinger, and Brien Flewelling. Direct image-to-likelihood for track-before-detect multi-bernoulli filter. *AIAA/AAS Spaceflight Mechanics Conference*, 2016.

[25] B-N Vo and W-K Ma. The gaussian mixture probability hypothesis density filter. *IEEE Transactions on signal processing*, 54(11):4091–4104, 2006.

[26] Kusha Panta, Ba-Ngu Vo, Sumeetpal Singh, and Arnaud Doucet. Probability hypothesis density filter versus multiple hypothesis tracking. In *Defense and Security*, pages 284–295. International Society for Optics and Photonics, 2004.

[27] B. Sease, B. Flewelling and J. Black. A class of convex optimization problems for template-based star subtraction. In *26th AIAA/AAS Spaceflight Mechanics Conference*, 2016.